2022 IEEE/RSJ International Conference on Intelligent Robots and Systems (IROS)
October 23-27, 2022, Kyoto, Japan

Systematic Evaluation and Analysis on Hybrid Strategies of Automatic Agent Last-mile Delivery

Xiaotong Zhang[1], Abdullatif Al Alsheikh[2] and Kamal Youcef-Toumi[1,2]

Abstract— **This paper focuses on problems associated with the deployment of automatic agents for last-mile delivery. We propose a framework and methodology to systematically evaluate and compare different hybrid strategies. Performance metrics in agent noise, delivery time, energy consumption, coverage rate, package throughput, and system costs are defined rigorously and modeled mathematically. Using the methodology, we conduct a case study in the city of Boston for four agent delivery strategies, including a hybrid strategy proposed in this paper. The proposed strategy utilizes available space in public transits' cabins during off-peak hours to relocate the agent traveling start locations. Simulations and analyses show that hybrid strategies outperform the Agent-Only delivery strategy in terms of noise exposure, energy consumption, and coverage rate. The performance of hybrid strategies highly depends on the characteristics of the ground transportation methods accompanying agents. Thus, the methods of ground transportation should carefully be examined and selected for each case and strategy in real-world applications.**

I. Introduction

Throughout the whole logistics process, the last-mile phase of the delivery is especially labor-intensive [1], costly [2], complex, unreliable, environmentally unfriendly [3], and time-consuming. Agent delivery is a potential solution to these problems by adopting robotic agents to complete the delivery tasks automatically and desirably without human intervention. The type of agents can be either unmanned flying agents or autonomous ground vehicles. Amazon, Alphabet-owned Wing, UPS, and FedEx all test intensively package or product delivery using drones to increase efficiency and reduce delivery costs [4], [5]. However, there is still a long way for practical large-scale deployment of the technology, especially in urban environments. Some of the problems are demonstrated in this paper, including noise pollution [6], aggregation of noise and traffic around the distribution centers, low coverage rates by battery limitations, and high energy consumption.

Several hybrid agent delivery strategies are proposed and developed for the sake of a solution necessary for practical large-scale agent delivery. The so-called hybrid strategies refer to a network of heterogeneous multi-typed agents teaming up to achieve the tasks collectively. The most well-developed hybrid strategy is the Agents with Trucks (AWT) strategy which combines conventional trucks and agents as each other's sidekicks [7], [8]. This strategy has been intensively studied in the aspects of hardware design, system integration [9], mathematical modeling [8], and routing and scheduling problems [10], [11], [12], [13]. Another category of hybrid strategies is to combine the agents with public transit systems. An example of these strategies is the Agents on Public Transits Delivery (AOPT) strategy. In AOPT, the agents can be piggybacked by the public transit vehicles, on which agents can rest to conserve energy and recharge themselves [14]. In this paper, another hybrid strategy, Agent-aided Public Transit Delivery (AAPT), is proposed and analyzed. In this strategy, the packages are transported by the spare space inside public transit cabins automatically. The agents are only involved in the last stage to transport packages to the final destinations from the nearest public transit stations.

An essential problem in the robotic last-mile delivery research is that systematic analysis and evaluation of these hybrid strategies based on a unified methodology are still lacking. On the one hand, previous studies on scheduling or routing problems of one specific strategy focused significantly on one or a few specific performance metrics of the system, such as delivery time [12], [15], [16], [17] and/or energy consumption [12], [16], [18]. Other metrics of the strategy are not well evaluated or studied, which may dramatically influence the efficiency and feasibility of the strategies, including noise pollution, working range, throughput, and system costs. On the other hand, previous research on performance metrics addressed the modeling or analysis of one specific metric instead of a systematic evaluation of hybrid strategies.

Two metrics, namely energy consumption and acoustic noise, attract more attention. Although the energy consumption modeling of drone delivery is still an active research area, Zhang et al. [19] carefully reviewed existing drone energy consumption models and categorized these models into integrated approaches and component approaches. Component approaches, which are used in this paper, decompose the energy consumption into either different sources or different flight phases, and sum up these components to achieve the desired fidelity. The analysis of noise propagation is much more complicated. Sound propagation modeling is mainly based on wave propagation theory [20]. And then, atmospheric effects, e.g. molecular absorption [21], wind and turbulence effects [22], Doppler effects [23], multi-path and diffraction [24], are augmented and integrated into the model. In addition to mathematical modeling, research on acoustic noise heavily rely on experiments. Noise signals from various drones, distances, velocities, surrounding conditions are mea-

[1] Department of Mechanical Engineering, Massachusetts Institute of Technology, Cambridge, MA, 02139, USA. kevxt@mit.edu, youcef@mit.edu

[2] Center for Complex Engineering Systems at KACST and MIT, Riyadh, Saudi Arabia. aalalsheikh@kacst.edu.sa

2022 IEEE/RSJ International Conference on Intelligent Robots and Systems (IROS) | 978-1-6654-7927-1/22/$31.00 ©2022 IEEE | DOI: 10.1109/IROS47612.2022.9981064

sured and analyzed in both temporal and frequency domains [25], [26]. However, the results from such experiments are difficult to generalize and adapt to a city scale. Thus, in this paper, a simplified noise propagation model is adapted to capture the main noise characteristics.

A systematic analysis and evaluation of different agent delivery strategies based on a unified framework are essential for the practical deployment of agent delivery. With this framework and methodology, the strategies can be compared with, and more resources can be inclined to a more competitive strategy. However, to the best of our knowledge, this work is the first to provide this understanding from a rigorous perspective. The main contributions of this paper are summarized as follows: 1) rigorous definitions of performance metrics with reasonable fidelity. We especially focus on the performance metrics that are still under active research or the ones that are vague and lacking a mathematical formulation; 2) a methodology to systematically analyze different hybrid agent delivery strategies within a unified framework; 3) a novel hybrid strategy combining the advantages of public transits and agent delivery; 4) sensitivity analyses of different factors on the performance of hybrid strategies, including the characteristics of the accompanying ground transportation systems.

II. Performance Evaluation Metrics

In this section, we introduce the definitions of metrics for the evaluation of different agent delivery strategies.

A. Agent Acoustic Noise

Acoustic noise from agents is the primary source of annoyance in the last-mile delivery. The modeling of agent noise is based on a simplified noise propagation model, which assumes point noise source and spherical propagation [20]. The noise intensity $I_i^{(x,y)}(t)$ at a given location (x, y), at time t and caused by the agent for the ith delivery task is

$$I_i^{(x,y)}(t) = \frac{P_i}{4\pi r_i(t)^2} \tag{1}$$

where P_i is the power of the noise source, $r_i(t)$ is the distance between point (x, y) and the noise source, t represents time, and the subscript i is the index of the delivery agent. Here, we assume that the parameters for each delivery task may be different because of different models of agents, payloads, weather conditions, and/or routes.

The annoyance of the agent noise and its corresponding health issues are influenced by both the intensity and duration of the noise. However, this relationship, which may be affected by the noise tone and the context during which the sound is heard, is still under active research [20]. Without loss of generality, we assume that noise annoyance grows linearly with the time duration. This assumption can be easily updated after a more accurate model. Thus, we define a metric called noise exposure $E_i^{(x,y)}$, which is defined for a specific task index i and location (x, y) as

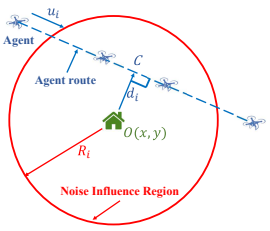

Fig. 1. Illustration of the noise influence region.

$$E_i^{(x,y)} \triangleq \int_0^{T_i^{(x,y)}} I_i^{(x,y)}(t)\ \mathrm{d}t \tag{2}$$

where $T_i^{(x,y)}$ is the noise duration for a specific location influenced by the ith delivery. $T_i^{(x,y)}$ is calculated as the time during which the agent is in the noise influence region illustrated in Fig. 1. When the agents operate outsides the noise influence region, we assume that the influence of agent noise is negligible. The noise influence region radius R_i is defined as

$$R_i = \sqrt{\frac{P_i}{4\pi I_a}} \tag{3}$$

where I_a represents the maximum allowable noise intensity. After substituting (1) in (2), the noise exposure is calculated to be

$$E_i^{(x,y)} \triangleq \int_0^{T_i^{(x,y)}} I_i^{(x,y)}(t)\ \mathrm{d}t \tag{4}$$

$$= \int_{\sqrt{{R_i}^2\ \ {d_i}^2}}^{\sqrt{{R_i}^2\ \ {d_i}^2}} \frac{P_i}{4\pi} \frac{1}{{d_i}^2 + z^2 + {h_i}^2} \frac{\mathrm{d}z}{u_i} \tag{5}$$

$$= \frac{P_i}{2\pi u_i \sqrt{{h_i}^2 + {d_i}^2}}\ tan^{-1}\left(\frac{\sqrt{{R_i}^2 - {d_i}^2}}{\sqrt{{h_i}^2 + {d_i}^2}}\right) \tag{6}$$

where d_i is the normal distance from (x, y) to the delivery route, u_i is the agent velocity; h_i is the agent working height, and z is the distance between the agent and point C in Fig. 1.

According to the guideline of CDC [27], "A one-time exposure to extreme loud sound or listening to loud sounds for a long time can cause hearing loss". Thus, three values based on the average value, maximum value and standard deviation should be carefully analyzed:

1) Average of the average noise exposure E_a: E_a is defined as

$$E_a = \frac{\iint \sum_{i=1}^{N} E_i^{(x,y)}\, \mathrm{d}x\, \mathrm{d}y}{S \cdot N} \tag{7}$$

where N is the number of total deliveries, S is the area of a region of interest. For example, S is the area of Boston, MA, in the United States of America for the case study in this paper. E_a reflects the average noise exposure performance within the region of interest, which significantly influences the residents' comfort.

2) Maximum of the average noise exposure E_m: E_m is defined as

$$E_m = \max_{(x,y)} \frac{\sum_{i=1}^{N} E_i^{(x,y)}}{N} \tag{8}$$

E_m reflects the noise performance of the worst location in terms of average noise exposures over a large number of delivery tasks.

3) Standard deviation of the average noise exposure E_s: E_s is defined as

$$E_s = \sigma \left(\frac{\sum_{i=1}^{N} E_i^{(x,y)}}{N} \right) \tag{9}$$

where σ represents the operation of calculating the standard deviation. E_s represents the uniformity of the average noise exposure within the region. This value is also critical in the following analysis to represent the aggregation of the noise exposure within a region.

The modeling of acoustic noise is simplified in this paper and can be improved in future research by incorporating more agent behavioral properties and/or geography-based properties of the surrounding environment.

B. Delivery Time

Delivery time reduction is a significant driving force for agent delivery. To assess the delivery time of different strategies, two key metrics are adopted, namely makespan M^k and average delivery time DT^k, where k represents the abbreviation of different strategies.

M^k is defined as:

$$M^k = \max_i M_i^k \tag{10}$$

where M_i^k is the time for strategy k to finish the delivery task i. Thus, makespan M^k represents the total time to finish all the deliveries with one strategy, which models the worst-case scenario or the guaranteed delivery time for a shipper using a specific strategy.

Average delivery time DT^k is defined as:

$$DT^k = \sum_{i=1}^{N} DT_i^k / N \tag{11}$$

where DT_i^k is the delivery time for the ith delivery task using strategy k. DT^k represents the average delivery time using one strategy.

C. Energy Consumption

Energy consumption of agent delivery is highly related to carbon emissions, operational cost, and operation range of agents. In this paper, we will use a component approach to decompose the energy consumption of the entire delivery journey into two components: energy consumption by agents EC_i^a, and energy consumption by ground transportation other than agents EC_i^g.

Ample research tried to address the modeling of agent energy consumption. In 2021, Zhang et al. systematically reviewed drone delivery energy consumption models. It is found that existing models adopt highly various modeling assumptions, and more studies are required to accurately reflect the energy consumption [19]. Thus. in this paper, data from empirical research and field experiments are used to calculate EC_i^a more accurately. The energy consumption EC_i^a is calculated as follows

$$EC_i^a = Epm^l \cdot d_i^l + Epm^u \cdot d_i^u \tag{12}$$

where Epm^l and Epm^u stands for energy per meter traveled in the condition of loaded and unloaded, respectively, and d_i^l and d_i^u are the loaded and unloaded travel distance of the ith delivery. The relationship between Epm^l and Epm^u can be derived using a simplified drone energy consumption model

$$Epm = \frac{(m_1 + m_2 + m_3)g}{\rho \cdot \eta} \tag{13}$$

where m_1, m_2 and m_3 represents the mass of the flying agent's structure, battery, and payload, respectively, g is the gravity acceleration, ρ is the lift-to-drag ratio, and η is the energy efficiency of the system. After assuming that the payload m_3 doesn't influence other parameters in (13), the relationship between Epm^u and Epm^l is

$$\frac{Epm^u}{m_1 + m_2} = \frac{Epm^l}{m_1 + m_2 + m_3} \tag{14}$$

D. Coverage Rate

The limitation of battery capacity poses the operation range limitation of agents. Thus, we propose a metric called Coverage Rate CR^k for strategy k. CR^k is defined as

$$CR^k = \frac{W^k}{N} \tag{15}$$

where N is the total number of delivery tasks in a given period of time of interest, and W^k is the number of packages within the working range WR_i^k of a strategy k and delivery task i. CR^k represents the percentage of delivery tasks, which can be delivered by strategy k even though the flying range of agents is limited by the battery capacity.

In some cases, only the value for unloaded flight range FR^k is unveiled by the manufacturer. Then the operational range given the same routes back can be derived using (14) to be

$$WR = \frac{FR \cdot Epm_u}{Epm_u + Epm_l} = \frac{FR \cdot (m_1 + m_2)}{2m_1 + 2m_2 + m_3} \tag{16}$$

E. Package Throughput

A main constraint of agent delivery is the low throughput of the system, especially for drone delivery, which in general has a very low load capacity per delivery.

The package throughput PT^k for a strategy k in a given period of time TI of interest can be calculated as

$$PT^k = \min_j f_j^k \cdot m_j^k \cdot TI \tag{17}$$

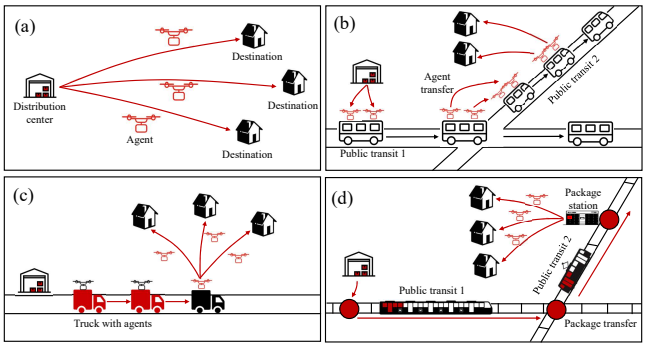

Fig. 2. Agent delivery strategies. (a) Agent-Only Delivery (AO); (b) Agents on Public Transits Delivery (AOPT); (c) Agents with Trucks Delivery (AWT); (d) Agent-Aided Public Transit Delivery (AAPT). Agents or other methods of transportation in red are the components carrying packages.

where j represents different methods of transportation in the system, f_j^k is the frequency of the transportation j, m_j^k is the number of packages carried by the transportation j once. The bottleneck methods of transportation in different strategies should be carefully examined and analyzed.

F. System Costs

Cost reduction is another driving force for automatic agent delivery. The analysis of system costs can be decomposed into two parts, i.e. operational costs OC and capital costs CC.

Operational costs are the costs accrued in the everyday operation, including energy consumption, data transmission, maintenance, labor, fees, etc. The performance of OC represents the cost performance in the long term.

Capital costs are one-time expenses incurred on the purchase of agents, lands, trucks, infrastructure reconstructions, etc. The value of CC reflects the costs required to make the system commercially operable.

III. Agent Delivery Strategies

After defining the metrics, four agent delivery strategies, whose working principles are illustrated in Fig. 2, are studied.

A. Existing Strategies

The first strategy, Agent-Only Delivery (AO), is the most common agent delivery method widely adopted. The agents carry the packages and travel directly between the distribution centers and the destinations, as illustrated in Fig. 2(a).

The two existing hybrid strategies shown in Fig. 2(b) and Fig. 2(c) are Agents on Public Transits Delivery (AOPT) and Agents with Trucks Delivery (AWT), which are well documented in [14] and [8]. The key idea in AOPT is to allow agents to be piggybacked on public transit vehicles. Thus the flying distance required for each delivery is dramatically reduced to alleviate the problems of AO. As for AWT, the agents and trucks work as each other's sidekicks. Trucks, serving as a moving warehouse in this strategy, carry not only the packages but also the agents that deliver the packages from the trucks to the destinations.

B. Agent-Aided Public Transit Delivery (AAPT)

Agent-Aided Public Transit Delivery (AAPT) is proposed in this paper, whose operation flow is shown in Fig. 2(d). In the first step, packages are transported by robots or trucks from the distribution centers to the nearest public transit stations. The packages are then unloaded and organized in a temporary storage. When the public transit arrives, the packages are automatically loaded into the public transit cabins. In the next step, the packages travel within the public transit systems, just like passengers. If necessary, the packages can even transfer between different public transits automatically. When the packages arrive at the stations that are the closest to the final destinations, the packages are unloaded from the public transits and either delivered directly to the customers or to another destination by agents.

The advantages of this strategy are apparent, especially for packages whose customers chose a slightly longer delivery time. Unlike other hybrid strategies, AAPT doesn't involve agents except for the last step. Thus, the agent numbers, agent traveling distances, energy consumptions, and noise emissions are dramatically reduced. Many people around the world are conscious about the future of our planet, and consequently make choices consistent with low emissions. Moreover, this system can maximally exploit the spare space and resources in public transits during off-peak hours.

Several factors may influence the feasibility and effectiveness of this system. In AAPT, we will need to augment the existing public transit systems with package stations and automatic package transfer mechanisms between different public transits. Moreover, the development of mechanisms to store packages within cabins without sacrificing passenger space and safety during peak hours is another challenge. Even though package stations with agents are already developed [28], the real-world deployment of AAPT still requires other technologies, which may impose intensive infrastructure reconstruction and substantial capital costs.

IV. Simulation Setup and Methods

A. Simulation Setup

We take Boston, MA, in the United States of America for the case study, and the setup is illustrated in Fig. 3. In the simulation, 3000 delivery tasks originating from the Amazon warehouse located at (-71.05417,42.39389) are generated uniformly within the boundary of Boston. The data of bus stops, bus routes, subway stations, and subway routes are downloaded from the government website of the state of Massachusetts [29], [30].

The type of agents in all the simulations are the same, an Amazon prime air delivery drone. Thus we assume $P_i = 1\ w$, which doesn't influence the comparison between strategies; $R_i = 500\ m$; $h_i = 121.92\ m$, which is the maximum FAA approved operation height for unmanned aircraft systems [31]; $u_i = 80\ km/h$ [32].

In the computation of energy consumption and coverage rate, we use the values of $Epm^l = 46.1\ J/m$, which is based on an experiment of the Amazon delivery drone [12]; $m_3 = 5$

lb [12], [33], $m_1 + m_2 = 55\ lb$ [32], [33]; $FR = 15\ miles$ [34]. Epm^u is calculated according to (14) to be 42.26 J/m. Moreover, we further assume $EC_i^g = 0\ J$ in this paper for simplicity. There are two reasons for $EC_i^g = 0\ J$: 1) if the strategy takes buses or subways as the methods of ground transportation, the marginal energy consumption for a 5 lb package is relatively low; 2) if the operation requires trucks, the energy consumption per package for diesel trucks are much lower than drones because of the high volume capacity of trucks, especially in cities with denser populations [35]. However, for a more precise comparison and analysis, this part of energy consumption should be modeled and taken into consideration. It is also worth mentioning that the use of diesel, and other fossil fuels, is scheduled to be reduced in the near future.

We make some assumptions to calculate the throughput: 1) the density of agents in operation in the city is limited to 4 within a 1 $km \times 1\ km$ square. Thus the number of agents in operation is limited to 928 for Boston; 2) for AOPT, the agents may use the roof of the entire vehicle (10 agents on one bus, and 40 agents on one subway); 3) for AAPT, agents can only take maximally one cabin of the subway (250 packages) or 20 % of each bus cabin (50 packages); 4) the operation time is from 8 am to 6 pm, 10 hours in total; 5) subway arrives every 6 minutes for one route ($f = 10/hour$), while bus arrives every 15 minutes for one route ($f = 4/hour$); 6) there are 7 subway lines and 70 bus routes. In the computation, $m_a = 1$ and $TI = 10$ hours for all the cases.

The methods of ground transportation in different hybrid strategies should be selected carefully. For AAPT, subways are used as shown in Fig. 2(d), and the package stations are installed at every subway station. Thus, the packages are only required to transfer between subways, which is much simpler and dramatically reduces the system complexity. As a fact, there are 8047 records of bus stops within the Massachusetts Bay Transportation Authority (MBTA) system [36], while there are only 149 subway stations as of 2019 [37].

For AOPT, buses are a better option, at least for Boston, as it may require the agents to take off to transfer between public transits, and subway routes in Boston are mostly underground. The underground part will prevent agents from taking off. Moreover, there are only 1148 active buses [38], which is much fewer than the bus stops. The modification cost for each bus is also much lower compared with the modification cost for each bus stop in AAPT.

However, in this paper, we will simulate AOPT and AAPT with both buses and subways to analyze the influence of different public transit methods on the performance of a strategy. The notations "-B" and "-S" after the strategy name denote the simulation with buses and subways, respectively.

B. Simulation Methods

The simulations and calculations of metrics proposed and defined in Section II rely on the derived agent routes, especially the takeoff and landing locations. The agent routes are the minor arcs of the great circles between the two locations. All distances in the simulations are the great-circle distances calculated using Vincenty's formulae [39]. For AO, the start points and destinations are the distribution center and package locations, respectively. In the simulation of AWT, a k-mean cluster algorithm is utilized to find the cluster centers, which are the destinations of trucks and the start points for agents. The detail of the algorithm is shown in [12] with the number of clusters set to be 30. The results of the clustering are shown in Fig. 3(b). For AOPT, the start points of agents for each package delivery are optimized globally along the public transit networks using a brute force search method, i.e. comparing the minimum distances from the destination to every route segment. For AAPT, the algorithm is similar to the one for AOPT, except that the brute force search only compares the distances from the destinations to public transit stations.

Noise pollution, energy consumption, and coverage rates can then be calculated based on the information of agent routes, agent traveling distances, and agent characteristics using the models in Section II. The calculations of package throughput are different and are based on the frequency and the package volume of agents in the network. The calculation details are described in Section V.

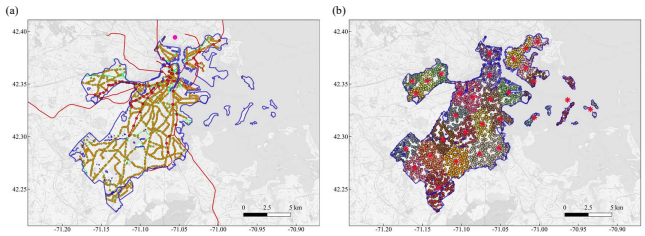

Fig. 3. Simulation Setup. Blue lines are the boundary of Boston. The purple dot is the Amazon warehouse. (a) Boston public transit infrastructure. Red lines, Green lines, red dots, and orange dots are the subway routes, bus routes, subway stations, and bus stops within Boston, respectively. (b) Clustered package delivery tasks. Different clusters are shown with different colors. Red stars are the cluster centers.

TABLE I
NOISE PERFORMANCE OF DIFFERENT STRATEGIES

Strategy	$E_a\ (w \cdot s/m^2)$	$E_m\ (w \cdot s/m^2)$	E_s
AO	$1.69{\cdot}10^{-6}$	$3.04{\cdot}10^{-5}$	$2.47{\cdot}10^{-6}$
AOPT-B	$4.99{\cdot}10^{-8}$	$1.26{\cdot}10^{-6}$	$6.88{\cdot}10^{-8}$
AOPT-S	$3.05{\cdot}10^{-7}$	$1.07{\cdot}10^{-5}$	$5.90{\cdot}10^{-7}$
AWT	$2.13{\cdot}10^{-7}$	$2.86{\cdot}10^{-6}$	$2.72{\cdot}10^{-7}$
AAPT-B	$5.28{\cdot}10^{-8}$	$1.03{\cdot}10^{-6}$	$6.11{\cdot}10^{-8}$
AAPT-S	$4.20{\cdot}10^{-7}$	$1.84{\cdot}10^{-5}$	$8.66{\cdot}10^{-7}$

V. Simulation Results and Strategy Analysis

A. Noise

The contour plots of average noise exposure are illustrated in Fig. 4. The values of E_a, E_m, and E_s are summarized in Table I. All three values for AO are the highest. The higher value of E_s represents the lower uniformity of noise exposure within the region, which agrees with Fig. 4(a) that the average noise exposure aggregates around the warehouse since a large portion of the deliveries travel through this area.

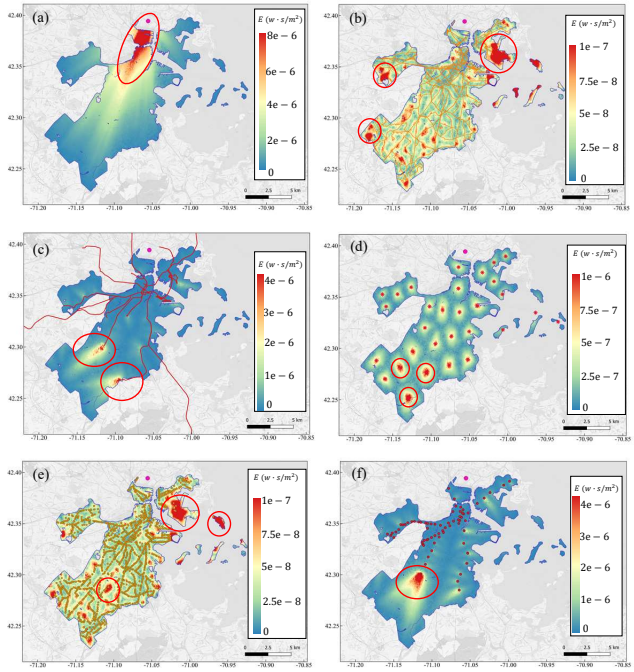

Fig. 4. Contour plots of average noise exposure of (a) AO; (b) AOPT-B; (c) AOPT-S; (d) AWT; (e) AAPT-B; (f) AAPT-S. Some high noise areas are highlighted with red circles. Orange lines in (b) and (e) are bus routes.

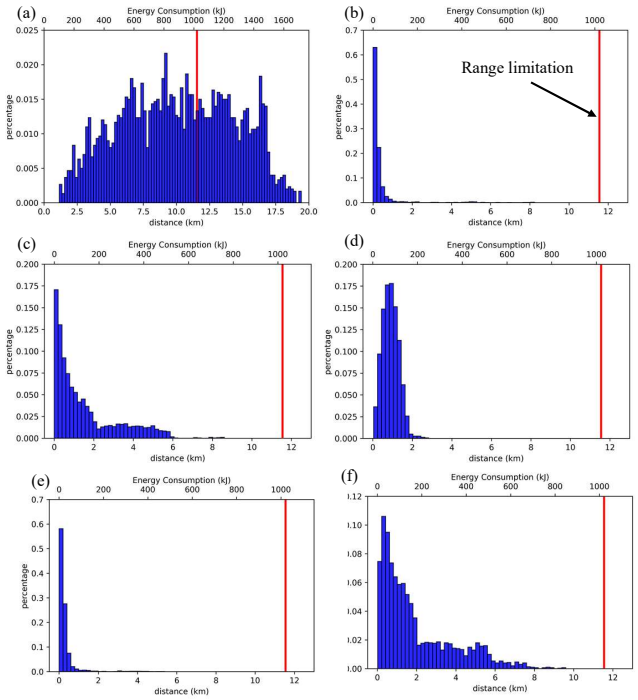

Fig. 5. Histograms of one-way agent traveling distance and EC_a of (a) AO; (b) AOPT-B; (c) AOPT-S; (d) AWT; (e) AAPT-B; (f) AAPT-S; . The red lines in the figure represent the range limitation of agents.

The performance of AOPT and AAPT is quite close. However, slight differences can still be noticed. In Table I, when using subways as the public transit method, AOPT outperforms AAPT in all three metrics. This is because that AOPT relaxes the constraints of AAPT that agents can only take off at the stations. When using buses in the systems, AAPT outperforms in the aspect of E_m and E_s.

The performance of AWT is worse than the cases using buses, but much better than the cases with subways. A slight aggregation of noise around the cluster centers is found.

Since AOPT-S can launch the agents not only at the stations but also along the routes, the aggregation in Fig. 4(f) for AAPT-S at the end station of the subway system is alleviated. Similarly, the aggregation in Fig. 4(e) highlighted with the red circle and caused by the suddenly enlarged gap between bus stops is also alleviated in Fig. 4(b).

B. Coverage Rate

Working range WR in the simulations is calculated to be 11.55 km according to (14) and (16). CRs for all strategies, except for AO, are calculated to be 100 %. CR^{AO} is only 60.60 %.

The histograms for the agent traveling distances are illustrated in Fig. 5. The average and maximum one-way agent traveling distances for different strategies are summarized in Table II. In Fig. 5, the distribution of AO is much uniform than other strategies, mainly spreading between 5 km and 17 km. The traveling distances of other strategies significantly aggregate close to 0 km, which means other methods of ground transportation travel much further than agents. It is

TABLE II

ONE-WAY AGENT TRAVELING DISTANCE AND ENERGY CONSUMPTION

Strategy	Average Distance (km)	Maximum Distance (km)	Mean EC_a (kJ)	Maximum EC_a (kJ)
AO	10.11	19.44	893.32	1717.72
AOPT-B	0.32	8.24	28.28	728.09
AOPT-S	1.52	8.61	134.31	760.78
AWT	0.90	2.83	79.52	250.06
AAPT-B	0.29	5.37	25.62	474.49
AAPT-S	1.99	9.60	175.84	848.26

demonstrated that the hybrid strategies dramatically reduce the required agent traveling distances by decentralizing and relocating the agent start locations.

For both AAPT and AOPT, cases using buses perform much better than those using subways as the bus routes and bus stops are much denser than subway routes and subway stations.

Though the average distance for AWT is longer than AAPT-B and AOPT-B, the maximum distance for AWT is much lower. This is because some areas are not covered by public transits, which requires a longer traveling distance from the public transit network to the destinations in these areas. However, AWT can allocate a cluster center after considering these areas and achieve a much lower maximum traveling distance.

C. Energy Consumption

The histograms of energy consumption EC^a for different strategies are also illustrated in Fig. 5 using the upper

TABLE III
STRATEGY PACKAGE THROUGHPUT CALCULATION

Strategy	f_a	PT_a	f_g	m_g	PT_g	PT
AO	3671.6	36716	-	-	-	36716
AOPT-B	116000	1160000	280	10	28000	28000
AOPT-S	24421.1	244211	70	40	28000	28000
AWT	41244.4	412444	-	-	-	412444
AAPT-B	128000	1280000	280	50	140000	140000
AAPT-S	18653.3	186533	70	250	175000	175000

axis. The average values and maximum values of EC^a are summarized in Table II. Since EC^a is proportional to the traveling distances in this case study, the trends and analyses of EC^a are almost similar to those for Coverage Rate CR.

D. Package Throughput

The computation of throughput is summarized in Table III. The subscript a and subscript g represents agents and ground transportation.

In the strategy of AO, there is no ground transportation involved. In the strategy of AWT, we assume that the shipper can adjust the number of trucks in the fleet subjectively. Thus the package throughput in these two strategies only depends on the agents.

The throughput of AO is the lowest since the traveling distance of agents in this strategy is too long. Given the number of operating agents is limited by the simulation assumption, the package throughput is limited. The throughput of AWT is the highest since it is not limited by the ground transportation. Moreover, the traveling distance for each package is much shorter because of the delivery trucks and the decentralization of start points. All other four strategies are limited by the throughput of ground transportation rather than agents. AAPT outperforms AOPT in the aspect of throughput since each subway or bus vehicle can take much more packages inside the cabins after careful arrangement than placing the bulky agents on top of the vehicles. The nature of AOPT that agents travel together with packages take too much space and reduces m_g and the throughput.

E. Delivery Time

The precise comparison of delivery time will require the exact solutions of the six cases. Thus for this metric, we only qualitatively analyze and compare the strategies.

Because AO directly delivers the packages to the customers, AO is the best for delivery time. AOPT-B should outperform AAPT-B since the transfer in AOPT is much more flexible and easier. AOPT only requires the agent to take off and land on a new public transit to complete the transfer. In contrast, AAPT will have to rely on the transfer mechanism at a public transit station. Similarly, AOPT-S should outperform AAPT-S.

However, the comparisons between AOPT-S and AOPT-B and between AAPT-S and AAPT-B depend on the characteristics and scheduling of public transit networks. Thus, it may require getting the exact solutions to continue the comparison. The analysis of AWT also requires solving the routing problem, which is one of our future research plans.

F. System Costs

System cost is a significant factor influencing the effectiveness of different strategies. However, the analysis of this factor is beyond the scope of this paper, which focuses on the technical part of the hybrid delivery strategies.

VI. CONCLUSION

In this paper, we present an effective and systematic methodology to evaluate different strategies of automatic agent delivery. With the help of mathematical modeling and simulations, we demonstrate that hybrid strategies outperform the Agent-Only (AO) strategy in terms of agent noise, coverage rate, and energy consumption. Moreover, it is validated that the characteristics of ground transportation in hybrid strategies dramatically influence the strategy performance. Last but not least, we propose a new hybrid agent delivery strategy, Agent-Aided Public Transit Delivery (AAPT), whose advantages in agent noise, energy consumption, coverage rate, and throughput are validated using the evaluation methodology proposed in this paper.

REFERENCES

[1] M. Joerss, F. Neuhaus, and J. Schröder, "How customer demands are reshaping last-mile delivery," *The McKinsey Quarterly*, vol. 17, pp. 1–5, 2016.

[2] L. Ranieri, S. Digiesi, B. Silvestri, and M. Roccotelli, "A review of last mile logistics innovations in an externalities cost reduction vision," *Sustainability*, vol. 10, no. 3, p. 782, 2018.

[3] J. Visser, T. Nemoto, and M. Browne, "Home delivery and the impacts on urban freight transport: A review," *Procedia-social and behavioral sciences*, vol. 125, pp. 15–27, 2014.

[4] "Amazon wins faa approval for prime air drone delivery fleet," https://www.cnbc.com/2020/08/31/amazon-prime-now-drone-delivery-fleet-gets-faa-approval.html, accessed: 2021-09-06.

[5] D. Bamburry, "Drones: Designed for product delivery," *Design Management Review*, vol. 26, no. 1, pp. 40–48, 2015.

[6] A. J. Torija, Z. Li, and R. H. Self, "Effects of a hovering unmanned aerial vehicle on urban soundscapes perception," *Transportation Research Part D: Transport and Environment*, vol. 78, p. 102195, 2020.

[7] H. Y. Jeong, B. D. Song, and S. Lee, "Truck-drone hybrid delivery routing: Payload-energy dependency and no-fly zones," *International Journal of Production Economics*, vol. 214, pp. 220–233, 2019.

[8] C. C. Murray and A. G. Chu, "The flying sidekick traveling salesman problem: Optimization of drone-assisted parcel delivery," *Transportation Research Part C: Emerging Technologies*, vol. 54, pp. 86–109, 2015.

[9] "Workhorse: The leader in last-mile delivery technology." https://workhorse.com/horsefly.htmll, accessed: 2022-02-22.

[10] N. Boysen, D. Briskorn, S. Fedtke, and S. Schwerdfeger, "Drone delivery from trucks: Drone scheduling for given truck routes," *Networks*, vol. 72, no. 4, pp. 506–527, 2018.

[11] D. Wang, P. Hu, J. Du, P. Zhou, T. Deng, and M. Hu, "Routing and scheduling for hybrid truck-drone collaborative parcel delivery with independent and truck-carried drones," *IEEE Internet of Things Journal*, vol. 6, no. 6, pp. 10 483–10 495, 2019.

[12] S. M. Ferrandez, T. Harbison, T. Weber, R. Sturges, and R. Rich, "Optimization of a truck-drone in tandem delivery network using k-means and genetic algorithm," *Journal of Industrial Engineering and Management (JIEM)*, vol. 9, no. 2, pp. 374–388, 2016.

[13] Y. S. Chang and H. J. Lee, "Optimal delivery routing with wider drone-delivery areas along a shorter truck-route," *Expert Systems with Applications*, vol. 104, pp. 307–317, 2018.

[14] S. Choudhury, K. Solovey, M. J. Kochenderfer, and M. Pavone, "Efficient large-scale multi-drone delivery using transit networks," *Journal of Artificial Intelligence Research*, vol. 70, pp. 757–788, 2021.

[15] D. Wang, P. Hu, J. Du, P. Zhou, T. Deng, and M. Hu, "Routing and scheduling for hybrid truck-drone collaborative parcel delivery with independent and truck-carried drones," *IEEE Internet of Things Journal*, vol. 6, no. 6, pp. 10 483–10 495, 2019.
[16] M. Marinelli, L. Caggiani, M. Ottomanelli, and M. Dell'Orco, "En route truck–drone parcel delivery for optimal vehicle routing strategies," *IET Intelligent Transport Systems*, vol. 12, no. 4, pp. 253–261, 2018.
[17] H. Y. Jeong, B. D. Song, and S. Lee, "Truck-drone hybrid delivery routing: Payload-energy dependency and no-fly zones," *International Journal of Production Economics*, vol. 214, pp. 220–233, 2019.
[18] D. Baek, Y. Chen, N. Chang, E. Macii, and M. Poncino, "Energy-efficient coordinated electric truck-drone hybrid delivery service planning," in *2020 AEIT International Conference of Electrical and Electronic Technologies for Automotive (AEIT AUTOMOTIVE)*. IEEE, 2020, pp. 1–6.
[19] J. Zhang, J. F. Campbell, D. C. Sweeney II, and A. C. Hupman, "Energy consumption models for delivery drones: A comparison and assessment," *Transportation Research Part D: Transport and Environment*, vol. 90, p. 102668, 2021.
[20] R. Kapoor, N. Kloet, A. Gardi, A. Mohamed, and R. Sabatini, "Sound propagation modelling for manned and unmanned aircraft noise assessment and mitigation: A review," *Atmosphere*, vol. 12, no. 11, p. 1424, 2021.
[21] H. E. Bass, L. C. Sutherland, A. J. Zuckerwar, D. T. Blackstock, and D. Hester, "Atmospheric absorption of sound: Further developments," *The Journal of the Acoustical Society of America*, vol. 97, no. 1, pp. 680–683, 1995.
[22] G. J. Ruijgrok, *Elements of aviation acoustics*. Delft University Press, 1993.
[23] R. Sabatini, T. Moore, and S. Ramasamy, "Global navigation satellite systems performance analysis and augmentation strategies in aviation," *Progress in aerospace sciences*, vol. 95, pp. 45–98, 2017.
[24] H. Bian, Q. Tan, S. Zhong, and X. Zhang, "Assessment of uam and drone noise impact on the environment based on virtual flights," *Aerospace Science and Technology*, vol. 118, p. 106996, 2021.
[25] C. E. Tinney and J. Sirohi, "Multirotor drone noise at static thrust," *Aiaa Journal*, vol. 56, no. 7, pp. 2816–2826, 2018.
[26] B. Schäffer, R. Pieren, K. Heutschi, J. M. Wunderli, and S. Becker, "Drone noise emission characteristics and noise effects on humans—a systematic review," *International Journal of Environmental Research and Public Health*, vol. 18, no. 11, p. 5940, 2021.
[27] "How does loud noise cause hearing loss?" https://www.cdc.gov/nceh/hearing_loss/how_does_loud_noise_cause_hearing_loss.html, accessed: 2021-09-06.
[28] "On-demand delivery platform," https://mttr.net/product, accessed: 2022-02-25.
[29] "Massgis data: Mbta bus routes and stops," https://www.mass.gov/info-details/massgis-data-mbta-bus-routes-and-stops, accessed: 2022-02-25.
[30] "Massgis data: Mbta rapid transit," https://www.mass.gov/info-details/massgis-data-mbta-rapid-transit, accessed: 2022-02-25.
[31] "Small unmanned aircraft systems (uas) regulations (part 107)," https://www.faa.gov/newsroom/small-unmanned-aircraft-systems-uas-regulations-part-107?newsId=22615, accessed: 2021-09-06.
[32] "Amazon to begin testing new delivery drones in the us," https://newatlas.com/amazon-new-delivery-drones-us-faa-approval/36957/, accessed: 2021-09-06.
[33] "Amazon's new delivery drone," https://www.mhlnews.com/transportation-distribution/article/22051164/amazons-new-delivery-drone, accessed: 2021-09-06.
[34] "Amazon wins faa approval for prime air drone delivery fleet," https://www.cnbc.com/2020/08/31/amazon-prime-now-drone-delivery-fleet-gets-faa-approval.html, accessed: 2021-09-06.
[35] T. Kirschstein, "Comparison of energy demands of drone-based and ground-based parcel delivery services," *Transportation Research Part D: Transport and Environment*, vol. 78, p. 102209, 2020.
[36] "Mbta bus stops," https://geo-massdot.opendata.arcgis.com/datasets/MassDOT::mbta-bus-stops-3/about, accessed: 2021-09-06.
[37] "List of mbta subway stations," https://en.wikipedia.org/wiki/List_of_MBTA_subway_stations, accessed: 2021-09-06.
[38] "The mbta vehicle inventory page," http://roster.transithistory.org/, accessed: 2021-09-06.
[39] "vincenty 0.1.4," https://pypi.org/project/vincenty/, accessed: 2022-02-25.